THE CUTTING EDGE

(Editor's Note: This quarterly column is compiled by JCO Technology Editor Ronald Redmond. To help keep our readers on The Cutting Edge, Dr. Redmond will spotlight a particular area of orthodontic technology every three months. Your suggestions for future subjects or authors are welcome.)

Steiner, Tweed, Ricketts—for most of us, these names conjure up memories of our orthodontic residencies and struggling to master cephalometric analysis. Steiner presented his system in 1953; today, there are dozens of cephalometric analyses that help us refine our diagnoses and treatment plans to fit individual patients. Orthodontists speak in a specialized language of ANB, FMA, and IMPA, which we have all come to accept and understand in daily communication. I smile when I think about the lively discussions that could be sparked once the new language was mastered.

Enter the new era with an even more powerful language: the third dimension. Dr. H. J. Cho presented a comprehensive 3D analysis in this column in 2009; in an effort to frame the new data sets, he encouraged the profession to consider a new cephalometric language. For most of us, though, new languages are difficult to comprehend. In this month's Cutting Edge article, Drs. Giampetro Farronato, Davide Farronato, Lucio Toma, and Francesca Bellincioni present a simplified 3D analysis. I suppose you could think of it as a primer—something to help us get started in our everyday practice. I'm certain that before long we will all have diagnostic discussions in the new language of "3D speak". Welcome to the beginning of the next 50 years.

W. RONALD REDMOND, DDS, MS

A Synthetic Three-Dimensional Craniofacial Analysis

Lateral cephalometric analysis has been used since the 1930s to evaluate dental and maxillofacial discrepancies and to assess changes from growth and treatment.[1] Although it has become the standard tool for orthodontic diagnosis and outcome appraisal,[2-13] the two-dimensional radiograph cannot accurately reflect three-dimensional physiological and pathological reality. Without a transverse dimension, plane geometry is inadequate for analysis of anatomic volumes.[14]

The introduction of cone-beam computed tomography (CBCT) of the maxillofacial region[15-18] has made 3D imaging more widely available for orthodontic applications.[19-22] CBCT datasets can


Dr. Redmond


Dr. G. Farronato


Dr. D. Farronato


Dr. Toma


Dr. Bellincioni

Dr. Giampietro Farronato is Director, Dr. Davide Farronato is a researcher, and Drs. Lucio Toma and Francesca Bellincioni are postgraduate students, School of Orthodontics, University of Milan, Via Commenda 10, 20122 Milan, Italy. E-mail Dr. Giampietro Farronato at giampietro.farronato@unimi.it.

Fig. 1 ANB angle and Wits appraisal traced on lateral cephalogram generated by cone-beam computed tomography (CBCT).

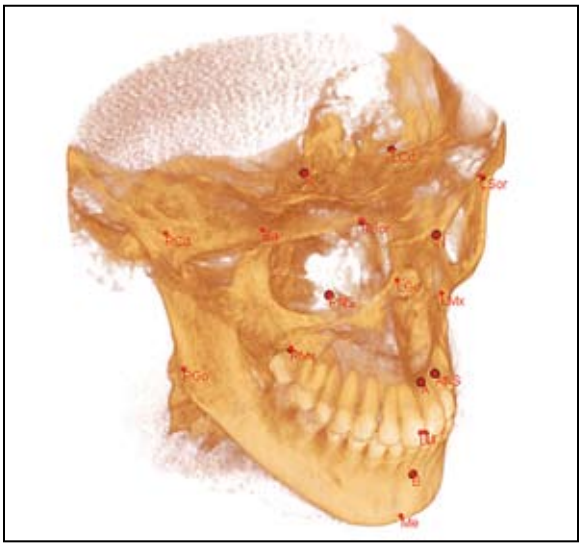

Fig. 2 Landmarks used for analysis.

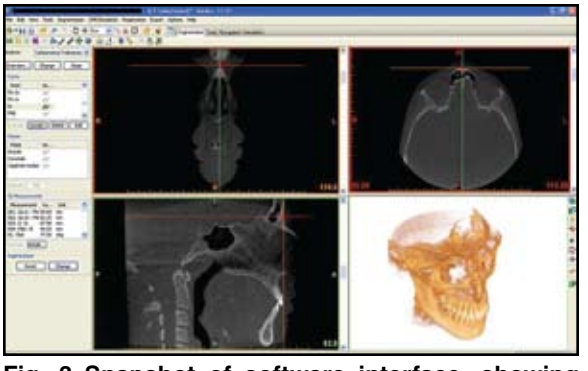

Fig. 3 Snapshot of software interface, showing landmark position on CT axial, coronal, and sagittal sections and on volumetric rendering.

be used to generate both 2D planar projections and 3D surface or volume renderings, opening new possibilities in diagnosis and treatment planning.

Previous CBCT-based orthodontic analyses have been based on single patients, or have required the identification of large numbers of landmarks and the use of complicated procedures.[23-30] This article presents a new, simplified approach to 3D CBCT evaluation. Although it does not provide a comprehensive assessment of dento-maxillofacial abnormalities, our approach allows clinicians to quickly identify major morphological anomalies by assessing relatively few landmarks.

Materials and Methods

We evaluated i-CAT* CBCT scans from 300 patients seen in the Department of Orthodontics, University of Milan, Italy. The scanning protocol involved a .4mm slice thickness, a 16cm × 22cm field of view, a 20-second scan time, and a .4mm voxel size. The raw data were saved in DICOM format and transferred to a central database.

For each patient, we traced the ANB angle and Wits appraisal on a CBCT-generated lateral cephalogram using 3Diagnosys** software (Fig. 1). The reproducibility and accuracy of these tracings have been found comparable to those of conventional cephalograms.[31-36] We classified each patient as having a Class I, II, or III skeletal relationship.

We then imported the DICOM data sets from a random selection of Class I cases (12 male and 18 female patients, age 7-67) into the Mimics program, version 11.11.*** Ten sagittal and eight lateral symmetrical landmarks were first identified in CT axial, coronal, or sagittal sections (Table 1, Fig. 2), and the location of each landmark was then confirmed in the other two sections. We also checked the position of each landmark on the 3D volumetric rendering generated by the program (Fig. 3).

*Registered trademark of Imaging Sciences International, 1910 N. Penn Road, Hatfield, PA 19440; www.imagingsciences.com.

**Registered trademark of 3DIEMME S.r.l., Via Risorgimento 9, 22063 Cantù, Italy; www.3diemme.it.

***Registered trademark of Materialise NV, Technologielaan 15, 3001 Leuven, Belgium; www.materialise.com.

TABLE 1
SKELETAL LANDMARKS USED IN ANALYSIS

Landmark	Description
A point	Point of maximum concavity in midline of maxillary alveolar process
Anterior nasal spine (ANS)	Most anterior midpoint of maxillary anterior nasal spine
B point	Point of maximum concavity in midline of mandibular alveolar process
Basion (Ba)	Most anterior point of foramen magnum
Condylion (L/R* Cd)	Most superior point of each mandibular condyle in sagittal and frontal planes
Gonion (L/R Go)	Point of maximum convexity at each mandibular angle
Lower incisor (LI)	Interproximal contact point between lower central incisors
Menton (Me)	Most inferior midpoint of chin on outline of mandibular symphysis
Maxillare (L/R Mx)	Intersection of maxillary alveolar process and maxillozygomatic process of maxilla
Nasion (N)	Midpoint of frontonasal suture
Posterior nasal spine (PNS)	Most posterior midpoint of posterior nasal spine on palatine bone
Sella (S)	Center of hypophyseal fossa (sella turcica)
Supraorbitale (L/R Sor)	Most superior point of upper external contour of orbital cavity
Upper incisor (UI)	Interproximal contact point between upper central incisors

*Left/Right.

Anteroposterior Landmarks

Mandibular body length (LGo-Me/RGo-Me): the distance between left and right gonion (Go) and menton (Me). A significant difference between the two values indicates primary anatomical asymmetry in the mandibular basal bone, which can influence the anteroposterior skeletal relationship.

Anterior cranial fossa length (S-N): the distance between sella (S) and nasion (N). A shorter S-N reflects a forward drift of the glenoid fossa (and therefore the condyle and mandible), whereas a longer S-N reflects a backward drift. All else being equal, these shifts can lead to Class III or Class II skeletal relationships, respectively.

Maxillary length (PNS-A): the distance between the posterior nasal spine (PNS) and A point. A longer or shorter maxilla can, of course, affect the anteroposterior skeletal relationship.

SNA: the angle formed between points S, N, and A, indicating the anteroposterior projection of the maxilla.

SNB: the angle formed between points S, N, and B, indicating the anteroposterior projection of the mandible.

ANB: the angle formed between points A, N, and B, indicating the anteroposterior intermaxillary relationship. In 3D analysis, unlike traditional cephalometrics, the difference between SNA and SNB often differs from the value of ANB. This can reflect the influence of the landmark positions on the *x*–axis and supply further information about spatial intermaxillary relationships.

Vertical Landmarks

Total anterior facial height (N-Me): the distance between N and Me.

Upper anterior facial height (N-ANS): the distance between N and the anterior nasal spine (ANS). In our sample, it represented 45% of the total facial height.

Lower anterior facial height (ANS-Me): the distance between ANS and Me. In our sample, it represented 55% of the total facial height, confirming the results of other studies.[11,14,37,38] In 3D analysis, these measurements represent actual heights, even in cases of asymmetry. In conventional cephalometric analysis, on the other hand, projection of an oblique line (as found in asymmetrical cases, where ANS and Me do not lie on the same sagittal plane), underestimates the true value.

Posterior facial height (S-LGo/S-RGo): the distance between S and left and right Go.

Mandibular ramus height (LCd-LGo/RCd-RGo): the distance between left and right condylion (Cd) and Go. A sizable difference between the two values indicates primary anatomic asymmetry. A short mandibular ramus (with a wider gonial angle) can lead to a Class II long-face pattern, whereas a long ramus can easily lead to a Class III situation.

Cranial base angle (Ba-S-N): the angle between basion (Ba), S, and N. A wider angle is generally associated with a Class II skeletal relationship, whereas a narrow angle is associated with a Class III relationship.

(continued on next page)

Craniomaxillary angle (SN-PNS-ANS): the angle between the floor of the anterior cranial fossa and the palatal plane. A narrowing angle can signify counterclockwise rotation of the palatal plane, which, in turn, can lead to widening of the gonial angle and clockwise rotation of the mandible, resulting in a tendency toward a Class II relationship. Conversely, a widening angle can be associated with a Class III relationship.

Craniomandibular angle (SN-LGo-Me/SN-RGo-Me): the angle between the floor of the anterior cranial fossa and the mandibular plane, measuring mandibular divergence. A difference between the two values can indicate asymmetry or mandibular rotation.

Maxillomandibular angle (PNS-ANS-LGo-Me/PNS-ANS-RGo-Me): the angle between the palatal and mandibular planes. A difference between the two values can indicate asymmetry or rotation of the skeletal bases, which can be confirmed by the other measurements.

Total gonial angle (LCd-LGo-Me/RCd-RGo-Me): the angle between the mandibular ramus and body. Differences indicate asymmetry, but may not necessarily indicate canting of the mandible in the frontal plane, since 3D measurements are not affected by the inclination of the analyzed structures. Widening or narrowing of this angle can influence the sagittal intermaxillary relationship.

Upper gonial angle (LCd-LGo-N/RCd-RGo-N) and lower gonial angle (N-LGo-Me/N-RGo-Me): can be used to predict mandibular growth, as shown in other studies[8]; the small sample size and lack of longitudinal data warrant caution with such interpretation.

Transverse Landmarks

These measurements investigate the symmetry (at different levels) of the face relative to a sagittal plane passing through Ba, S, and N (Fig. 4). The reference landmarks were chosen because of their high reproducibility.[39] Linear values are only indicative; much more important is the difference between the two sides of the face.

Supraorbitale to sagittal plane (LSor-RSor-Sag P): the distance between the superior margin of each orbital cavity (Sor) and the sagittal plane of symmetry (Sag P).

Maxillare to sagittal plane (LMx-RMx-Sag P): the distance between each maxillare (Mx) and Sag P.

Condylion to sagittal plane (LCd-RCd-Sag P): the distance between the superior margin of each mandibular condyle and Sag P.

Gonion to sagittal plane (LGo-RGo-Sag P): the distance between each mandibular angle and Sag P.

Upper incisor midline and lower incisor midline to sagittal plane (UI-Sag P, LI-Sag P): the distances between the superior and inferior dental midlines and Sag P.

Landmark identification provided 36 linear and angular measurements in the vertical, sagittal, and transverse planes (see box).

We used R statistical computing software, version 2.11.0,† to analyze the data. We calculated the mean, standard deviation, standard error of the mean, and 95% confidence interval for each measurement within the group of 30 Class I patients (Table 2).

Discussion

Although cephalometric analysis has long been the basis of orthodontic diagnosis, it has several limitations:

- A 2D analysis cannot accurately describe the 3D complexity of dentomaxillofacial discrepancies.
- Superimpositions prevent visualization of the internal structures of the craniomaxillofacial region. Moreover, it is often impossible to distinguish the left and right sides of the skull.
- Radiographic interpretation and landmark identification are challenging, even for experienced clinicians.
- Patient positioning is critical; any translation or

†R Project for Statistical Computing, Wirtschaftsuniversität Wien, Augasse 2-6, 1090 Vienna, Austria; www.r-project.org.

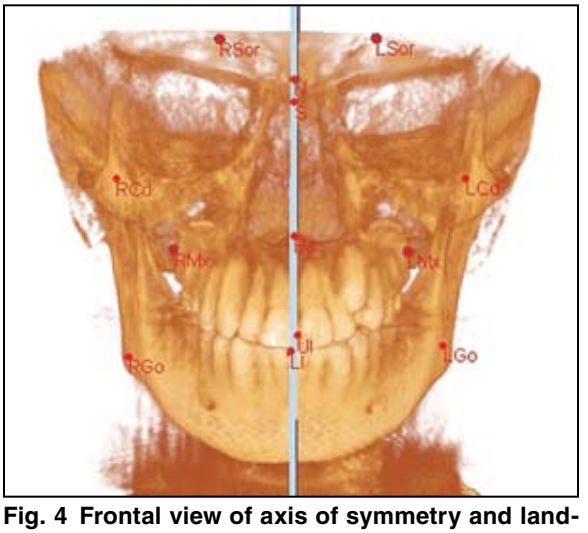

Fig. 4 Frontal view of axis of symmetry and landmarks used for transverse analysis.

TABLE 2
3D CRANIOFACIAL ANALYSIS OF SUBJECTS WITH CLASS I SKELETAL RELATIONSHIPS

Variable	Mean	S.D.	SEM	95% CI
LGo-Me	79.29mm	6.59mm	1.20mm	76.83-81.75mm
RGo-Me	79.12mm	6.27mm	1.15mm	76.77-81.46mm
S-N	65.30mm	3.67mm	0.67mm	63.93-66.67mm
PNS-A	45.71mm	3.63mm	0.66mm	44.35-47.06mm
SNA	81.25°	2.88°	0.53°	80.17-82.32°
SNB	78.47°	2.96°	0.54°	77.34-79.58°
ANB	3.05°	0.95°	0.17°	2.69-3.40°
N-Me	107.42mm	8.39mm	1.53mm	104.29-110.55mm
N-ANS	49.10mm	4.14mm	0.76mm	47.56-50.65mm
N-ANS proportion	45.0%	2.0%	0.3%	45.0-46.0%
ANS-Me	59.55mm	5.17mm	0.95mm	57.62-61.48mm
ANS-Me proportion	55.0%	2.0%	0.4%	55.0-56.0%
S-LGo	81.74mm	8.60mm	1.57mm	78.53-84.95mm
S-RGo	82.52mm	8.55mm	1.56mm	79.33-85.72mm
LCd-LGo	51.66mm	6.95mm	1.27mm	49.06-54.25mm
RCd-RGo	52.40mm	6.86mm	1.25mm	49.84-54.96mm
Ba-S-N	129.30°	4.95°	0.90°	127.45-131.14°
SN-PNS-ANS	8.11°	3.00°	0.55°	6.99-9.23°
SN-LGo-Me	45.85°	4.23°	0.77°	44.27-47.43°
SN-RGo-Me	45.24°	4.68°	0.85°	43.50-46.99°
PNS-ANS-LGo-Me	40.80°	3.07°	0.56°	39.66-41.94°
PNS-ANS-RGo-Me	40.78°	3.51°	0.64°	39.47-42.09°
LCd-LGo-Me	119.40°	6.84°	1.25°	116.84-121.95°
RCd-RGo-Me	118.61°	6.97°	1.27°	116.01-121.21°
LCd-LGo-N	54.44°	4.70°	0.86°	52.69-56.20°
RCd-RGo-N	54.19°	4.73°	0.86°	52.42-55.95°
N-LGo-Me	65.23°	4.23°	0.77°	63.65-66.81°
N-RGo-Me	64.77°	4.42°	0.81°	63.12-66.42°
△ LSor-RSor-Sag P	2.57mm	1.98mm	0.36mm	1.83-3.31mm
△ LMx-RMx-Sag P	3.16mm	2.78mm	0.51mm	2.12-4.19mm
△ LCd-RCd-Sag P	1.61mm	1.82mm	0.33mm	0.93-2.29mm
△ LGo-RGo-Sag P	3.80mm	4.01mm	0.73mm	2.30-5.29mm
UI-Sag P	2.60mm	2.10mm	0.38mm	1.81-3.38mm
LI-Sag P	4.04mm	6.87mm	1.25mm	1.48-6.61mm

rotation of the head can cause variability in cephalometric measurements.

CBCT avoids all these drawbacks. With no landmark superimpositions or errors related to patient positioning, relatively low radiation doses, and the ability of some software to obtain accurate measurements from reconstructed images, 3D digital imaging systems continue to gain popularity and are increasingly the focus of research.

Rather than generating a comprehensive description of the intricate three-dimensional interrelationships among dentomaxillofacial discrepancies, the aim of our analysis is to direct the clinician's attention toward the most important craniofacial region and provide the elements needed to identify involved structures quickly and reliably. The strength of this analytical method is its simplicity. Few landmarks are needed, and little time is required compared to previous techniques, making it possible to apply this method in everyday practice. In addition, it paves the way for further research, specifically on normal criteria for 3D analyses and the 3D features of the principal dysmorphic categories.

REFERENCES

1. Broadbent, B.H.: A new x-ray technique and its application to orthodontia, Angle Orthod. 1:45-66, 1931.
2. Tweed, C.H.: The Frankfort-mandibular plane angle in orthodontic diagnosis, classification, treatment planning and prognosis, Am. J. Orthod. 32:175-230, 1946.
3. Björk, A.: The face in profile: An anthropological x-ray investigation on Swedish children and conscripts, Svensk Tandläkare Tidskrift 40, 1947.
4. Steiner, C.C.: Cephalometrics for you and me, Am. J. Orthod. 39:729-755, 1953.
5. Downs, W.B.: Analysis of the dentofacial profile, Angle Orthod. 26:191-212, 1956.
6. Sassouni, V.: Diagnosis and treatment planning via roentgenographic cephalometry, Am. J. Orthod. 44:433-463, 1958.
7. Ricketts, R.M.: Cephalometric analysis and synthesis, Angle Orthod. 31:141-156, 1961.
8. Jarabak, J.R. and Fizzell, J.A.: *Technique and Treatment with Lightwire Edgewise Appliance*, C.V. Mosby Co., St. Louis, 1972.
9. Burstone, C.J.; James, R.B.; Legan, H.; Murphy, G.A.; and Norton, L. A.: Cephalometrics for orthognathic surgery, J. Oral Surg. 36:269-277, 1978.
10. Legan, H.L. and Burstone, C.J.: Soft tissue cephalometric analysis for orthognathic surgery, J. Oral Surg. 38:744-751, 1980.
11. Delaire, J.; Schendel, S.A.; and Tulasne, J.F.: An architectural and structural craniofacial analysis: A new lateral cephalometric analysis, Oral Surg. Oral Med. Oral Pathol. 52:226-238, 1981.
12. Holdaway, R.A.: A soft-tissue cephalometric analysis and its use in orthodontic treatment planning, Part I, Am. J. Orthod. 84:1-28, 1983.
13. McNamara, J.A. Jr.: A method of cephalometric evaluation, Am. J. Orthod. 86:449-469, 1984.
14. Delaire, J.: [Craniofacial architectural equilibrium in orthodontics and orthognathic surgery], Orthod. Fr. 56:353-364, 1985.
15. Scarfe, W.C. and Farman, A.G.: What is cone-beam CT and how does it work? Dent. Clin. N. Am. 52:707-730, 2008.
16. De Vos, W.; Casselman, J.; and Swennen, G.R.: Cone-beam computerized tomography (CBCT) imaging of the oral and maxillofacial region: A systematic review of the literature, Int. J. Oral Maxillofac. Surg. 38:609-625, 2009.
17. Farman, A.G. and Scarfe, W.C.: The basics of maxillofacial cone beam computed tomography, Semin. Orthod. 15:2-13, 2009.
18. Tetradis, S. and White, S.C.: A decade of cone beam computed tomography, J. Calif. Dent. Assoc. 38:24-26, 2010.
19. Kau, C.H.; Richmond, S.; Palomo, J.M.; and Hans, M.G.: Three-dimensional cone beam computerized tomography in orthodontics, J. Orthod. 32:282-293, 2005.
20. Hechler, S.L.: Cone-beam CT: Applications in orthodontics, Dent. Clin. N. Am. 52:809-823, 2008.
21. Grauer, D.; Cevidanes, L.S.; and Proffit, W.R.: Working with DICOM craniofacial images, Am. J. Orthod. 136:460-470, 2009.
22. Merrett, S.J.; Drage, N.A.; and Durning, P.: Cone beam computed tomography: A useful tool in orthodontic diagnosis and treatment planning, J. Orthod. 36:202-210, 2009.
23. Bettega, G.; Payan, Y.; Mollard, B.; Boyer, A.; Raphael, B.; and Lavallée, S.: A simulator for maxillofacial surgery integrating 3D cephalometry and orthodontia, Comput. Aided Surg. 5:156-165, 2000.
24. Olszewski, R.; Cosnard, G.; Macq, B.; Mahy, P.; and Reychler, H.: 3D CT-based cephalometric analysis: 3D cephalometric theoretical concept and software, Neuroradiol. 48:853-862, 2006.
25. Terajima, M.; Yanagita, N.; Ozeki, K.; Hoshino, Y.; Mori, N.; Goto, T.K.; Tokumori, K.; Aoki, Y.; and Nakasima, A.: Three-dimensional analysis system for orthognathic surgery patients with jaw deformities, Am. J. Orthod. 134:100-111, 2008.
26. Cho, H.J.: A three-dimensional cephalometric analysis, J. Clin. Orthod. 43:235-252, 2009.
27. Treil, J.; Casteigt, J.; Borianne, P.; and Faure, J.: [3D cephalometry], Orthod. Fr. 71:153-154, 2000.
28. Treil, J.; Waysenson, B.; Borianne, P.; Casteigt, J.; Faure, J.; and Horn, A.: Three-dimensional cephalometry, Alpha Omegan 94:34-39, 2001.
29. Swennen, G.J.; Schutyser, F.A.; and Hausamen, J.E.: *Three Dimensional Cephalometry: A Color Atlas and Manual*, Springer, Berlin, 2005.
30. Swennen, G.R.; Mollemans, W.; and Schutyser, F.: Three-dimensional treatment planning of orthognathic surgery in the era of virtual imaging, J. Oral Maxillofac. Surg. 67:2080-2092, 2009.
31. Kumar, V.; Ludlow, J.B.; Mol, A.; and Cevidanes, L.: Comparison of conventional and cone beam CT synthesized cephalograms, Dentomaxillofac. Radiol. 36:263-269, 2007.
32. Moshiri, M.; Scarfe, W.C.; Hilgers, M.L.; Scheetz, J.P.; Silveira, A.M.; and Farman, A.G.: Accuracy of linear measurements from imaging plate and lateral cephalometric images derived from cone-beam computed tomography, Am. J. Orthod. 132:550-560, 2007.
33. Cattaneo, P.M.; Bloch, C.B.; Calmar, D.; Hjortshøj, M.; and Melsen, B.: Comparison between conventional and cone-beam computed tomography-generated cephalograms, Am. J. Orthod. 134:798-802, 2008.
34. Periago, D.R.; Scarfe, W.C.; Moshiri, M.; Scheetz, J.P.; Silveira, A.M.; and Farman, A.G.: Linear accuracy and reliability of cone beam CT derived 3-dimensional images constructed using an orthodontic volumetric rendering program, Angle Orthod. 78:387-395, 2008.
35. Berco, M.; Rigali, P.H. Jr.; Miner, R.M.; DeLuca, S.; Anderson, N.K.; and Will, L.A.: Accuracy and reliability of linear cephalometric measurements from cone-beam computed tomography scans of a dry human skull, Am. J. Orthod. 136:17e11-19, 2009.
36. Moreira, C.R.; Sales, M.A.; Lopes, P.M.; and Cavalcanti, M.G.: Assessment of linear and angular measurements on three-dimensional cone-beam computed tomographic images, Oral Surg. Oral Med. Oral Pathol. Oral Radiol. Endod. 108:430-436, 2009.
37. Brodie, A.G.: Some recent observations on the growth of the face and their implications to the orthodontist, Am. J. Orthod. 26:741-757, 1940.
38. Wylie, W.L.: The relationship between ramus height, dental height, and overbite, Am. J. Orthod. 32:57-67, 1946.
39. Muramatsu, A.; Nawa, H.; Kimura, M.; Yoshida, K.; Maeda, M.; Katsumata, A.; Ariji, E.; and Goto, S.: Reproducibility of maxillofacial anatomic landmarks on 3-dimensional computed tomographic images determined with the 95% confidence ellipse method, Angle Orthod. 78:396-402, 2008.